Electronic and optical properties of hafnia polymorphs

T.V. Perevalov *, M.V. Ivanov, V.A. Gritsenko

Institute of Semiconductor Physics, 13 Lavrentieva Ave, 630090 Novosibirsk, Russia

ABSTRACT

The band structure, dielectric constants and linear optical properties of the cubic, tetragonal and monoclinic HfO$_2$ were calculated within density functional methods. The calculation were performed with both standard and hybrid density functionals which accurately reproduce the experimental band gaps. Electronic structures of hafnia polymorphs with oxygen vacancies were investigated. It was found out, that oxygen vacancy can be both electron and hole trap in HfO$_2$.

© 2011 Elsevier B.V. All rights reserved.

1. Introduction

Hafnia (HfO$_2$) is a wide band gap material, with a high dielectric constant, which has wide applications in optical and protective coating technology. HfO$_2$ is the promising material to replace SiO$_2$ as gate isolator in metal-oxide semiconductor devices [1,2]. These applications require knowledge of its electronic and optical properties. A number of first-principles studies have been dedicated to HfO$_2$. Because monoclinic (m-) HfO$_2$ is stable at room temperature its properties are more investigated than properties of tetragonal (t-) or cubic (c-) HfO$_2$. Moreover, most of early electronic structure calculations of hafnia were based on standard density-functional theory (DFT) methods, which suffer from well-known band-gap underestimation problem.

Oxygen vacancies are dominating intrinsic defects in the bulk of many high-k oxides including HfO$_2$ and are also thought to be presented in high concentrations in thin films [1]. However, in spite of numerous experimental studies, the role of oxygen vacancies in HfO$_2$ is still circumstantial. For instance, the measured defect energy levels differ considerably among the various experiments.

2. Methods

We have performed calculations in the framework of DFT using the *ab initio* simulation code QUANTUM-ESPRESSO. We have exploited both the exchange–correlation potential of the generalized gradient approximation (GGA) as approximated by the Burke–Perdew and hybrid functional HSE. The valence electronic eigenfunctions were obtained from an expansion in plane waves, while the core electrons were replaced by the norm-conserving pseudopotentials. To study dielectric permittivity, linear response methods based on DFT were employed to obtain Born effective charges and infrared active phonon modes at zone center. Then the static dielectric tensor can be calculated as follows:

$$\varepsilon_{\alpha\beta}^0 = \varepsilon_{\alpha\beta}^\infty + \frac{4\pi}{M_0 V} \sum_\lambda \frac{\tilde{z}_{\lambda\alpha}^* \tilde{z}_{\lambda\beta}^*}{\omega_\lambda^2}.$$

Here the $\tilde{Z}_{\lambda\alpha}^*$ are mode effective charges, M_0 is a reference mass that is taken to be 1 amu, ω_λ is the frequency of the λ IR-active phonon mode, V is the volume of the unit cell.

The periodic supercell approach was used for the simulation of the oxygen vacancy. Oxygen vacancies in c-, t- and m-HfO$_2$ were created in 81, 108 and 96 atoms supercells respectively, with the following atomic positions relaxation. The charge localization energies were estimated as difference between perfect and defect supercell electron/hole affinities, as follows:

$$\Delta\varepsilon^{e/h} = (E_{perfect}^{q=-1/+1} - E_{perfect}^{q=0}) - (E_{defect}^{q=-1/+1} - E_{defect}^{q=0}).$$

3. Results

The calculated fully relaxed crystal structures of c-, t- and m-HfO$_2$ agree very well with experimental data available in literature. The band gaps of hafnia polymorphs calculated within standard and hybrid DFT are compared to experimental values in Table 1. It is seen, that hybrid DFT gives energy gaps that better agree with experimental values. Fig. 1 demonstrates the band structures of c-, t- and m-HfO$_2$ calculated within hybrid DFT.

The carrier effective masses and the complex dielectric function were obtained from the band structure. Table 2 presents calculated values of band effective masses of electrons and holes in hafnia polymorphs. In c- and t-HfO$_2$ both – light and heavy electrons and holes are presented, whereas m-HfO$_2$ shows only heavy charge carriers. The electron effective masses are shown to be several

* Corresponding author.
E-mail address: timson@isp.nsc.ru (T.V. Perevalov).

Table 1
Band gaps of HfO$_2$ polymorphs obtained in this work compared to the experimental data.

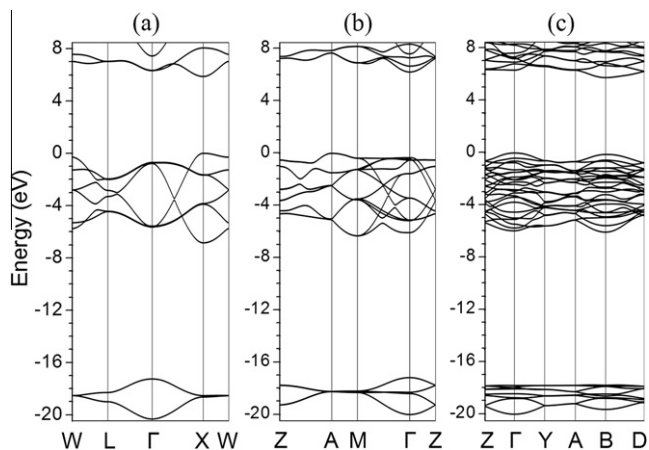|	c-HfO$_2$	t-HfO$_2$	m-HfO$_2$
DFT (eV)	3.4	4.0	3.6
Hybrid DFT (eV)	5.5	6.1	5.6
Experiment (eV)	5.8[4]	–	5.68[5]

Fig. 1. Band structures along the high-symmetry lines of the Brillouin Zone of cubic (a), tetragonal (b) and monoclinic (c) HfO$_2$ calculated with hybrid DFT.

Table 2
The effective electron m_e^* and hole m_h^* masses and corresponding Brillouin zone directions for HfO$_2$ polymorphs. The numbers in parentheses correspond to mass values obtained from hybrid DFT calculations.

	c-HfO$_2$	t-HfO$_2$	m-HfO$_2$
$\dfrac{m_e^*}{m_0}$	0.8 (1.0) Γ-L 1.9 (2.5) Γ-X 0.5 (0.6) Γ-X	0.6 (0.8) Γ-M 1.9 (0.9) Γ-Z	1.1 (1.3) B-A 1.7 (2.1) B-D
$\dfrac{m_h^*}{m_0}$	0.3 (0.4) X-Γ` 3.1 (2.7) X-W	0.8 (0.6) A-Z 3.6 (2.6) A-M	1.6 (2.3) Γ-Z 1.8 (1.7) Γ-Y

times heavier than the electron tunneling effective mass in amorphous HfO$_2$ [3].

Figs. 2 and 3 show the averaged imaginary and real parts of the complex dielectric function of HfO$_2$ polymorphs calculated using the hybrid DFT. The origins of the different peaks in the calculated dielectric functions can be deduced in terms of interband transitions. The calculated imaginary and real dielectric functions for cubic HfO$_2$ are in good agreement with the experimental data reported in [4] for energies in range 4.5–9.5 eV using UV ellipsometry spectroscopy.

The calculated electronic (ε^∞) and lattice (ε^{latt}) dielectric permittivity constants are presented in Table 3. Lattice dielectric permittivities were calculated only in standard DFT approach. The static dielectric tensor is diagonal and isotropic in the cubic phase. Due to the tetragonal symmetry of t-HfO$_2$, this tensor is also diagonal, but it has two independent components $\varepsilon_{xx} = \varepsilon_{yy}$ and ε_{zz}. The m-HfO$_2$ has four independent components of permittivity tensor: $\varepsilon_{xx}, \varepsilon_{yy}, \varepsilon_{zz}$ and ε_{xz}. It is seen, that the calculated dielectric constants vary widely from phase to phase. The t-HfO$_2$ has the highest dielectric constants relative to other phases. The results agree with previous calculated data [6,7]. As there are few experimental investigations of dielectric properties of crystalline hafnia, comparison of calculated dielectric constants with experimental values may not be possible.
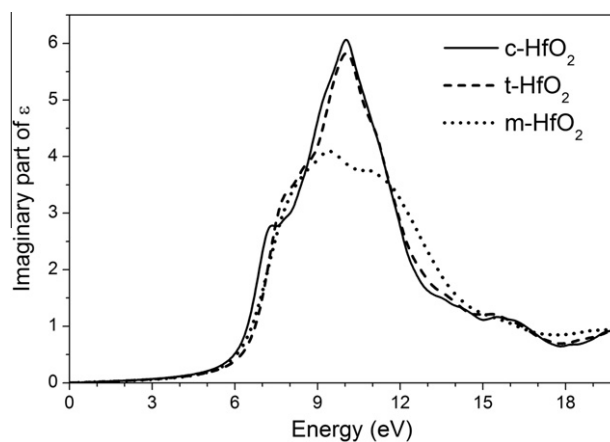

Fig. 2. Calculated with hybrid DFT imaginary part of the dielectric function for cubic (bold line), tetragonal (dash line) and monoclinic (dot line) HfO$_2$.
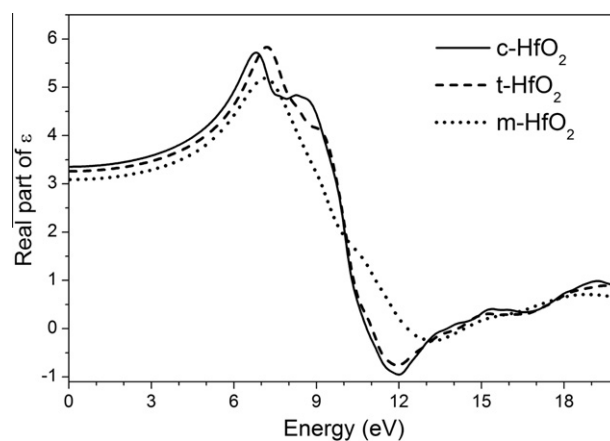

Fig. 3. Calculated with hybrid DFT real part of the dielectric function for cubic (bold line), tetragonal (dash line) and monoclinic (dot line) HfO$_2$.

Table 3
Calculated the optical and static dielectric constants of HfO$_2$ polymorphs. The numbers in parentheses correspond to values obtained from hybrid DFT calculations.

	c-HfO$_2$		t-HfO$_2$		m-HfO$_2$	
	ε^∞	ε^{latt}	ε^∞ $\perp, \parallel$	ε^{latt}	ε^∞ xx, yy, zz	ε^{latt}
DFT	5.1	20.4	5.1 4.7	42.0 11.2	4.9 4.7 4.5	6.4 12.0 6.6
Hybrid DFT	3.3	–	3.3 3.2	–	3.2 3.1 3.0	–
Ref. [6]	5.37	20.8	5.13 5.39	14.87 27.42	–	–
Ref. [7]	–	23.9	–	92.3 10.7	–	13.1 10.8 7.53

The calculated partial density of states (PDOS) spectra for hafnia polymorphs demonstrate that neutral oxygen vacancy create one gap state into the band gap which is doubly occupied (Fig. 4). This level lies above the valence band edge at 2.5 eV in standard DFT and at 3.2 eV in hybrid DFT calculations. It should be noted that another theoretical researches which give improved band gaps show wide range of neutral oxygen vacancy level position: 2.9 eV
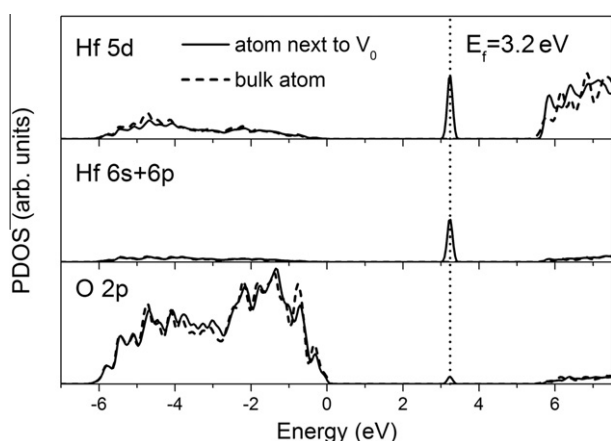
Fig. 4. Calculated with hybrid DFT partial density of states of adjacent Hf and O ion at the O vacancy in m-HfO$_2$.
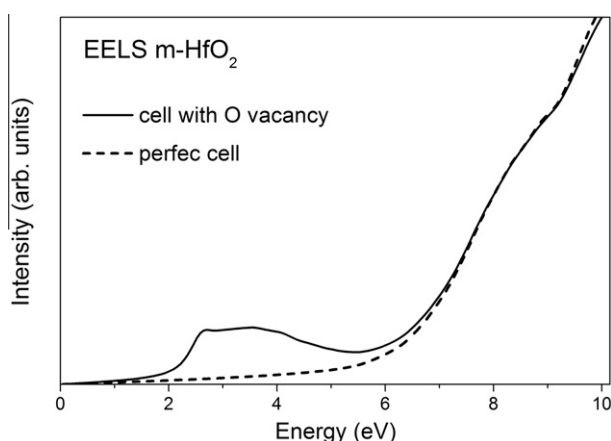

Fig. 5. Calculated with hybrid DFT ELS spectra for m-HfO$_2$ with oxygen vacancy (solid line) in compared with perfect structure (dashed line).

[8], 3.1 eV [9] and 3.8 eV [10] above the hafnia valence band top. The second vacancy state is also found in the density of states at about 6 eV in Fig. 4, essentially at the conduction band.

The calculated ELS spectrum (i.e. $-Im 1/\varepsilon$) of m-HfO$_2$ supercell with oxygen vacancy shows a wide absorption peak at 2.5–4.0 eV, which is attributed to an oxygen vacancy (Fig. 5). This result is compared with experimental absorption peak that exists in the range 4.5–5.0 eV in absorption spectra $(\alpha h \nu n)^{1/2}$ for polycrystalline HfO$_2$ [11]. The discrepancy is required the following investigations.

The charge localization energies on oxygen vacancy in hafnia polymorphs were calculated within simple DFT. It was obtained that electron and hole capture on oxygen vacancy is energetically favorable process. The energy gain for electron capture is 0.1 eV, 0.2 eV, 0.1 eV, whereas energy gain for hole capture is 2.7 eV, 2.7 eV, 2.6 eV for c-, t- and m-HfO$_2$ respectively. That results indicate that neutral oxygen vacancy in hafnia produces shallow donor energy level, but this fact disagrees with previous investigations [12]. It could be explained that DFT gave incorrect description of excited states in solids. Nevertheless our results afford ground for conclusion that oxygen vacancy in hafnia can play role of charge localization center.

4. Conclusions

The electronic and optical properties of c-, t- and m-HfO$_2$ were calculated within standard and hybrid DFT. The band structures, dielectric constants and optical properties are in reasonable agreement with previous simulations and available experimental results. The calculated effective electron and hole masses, and dielectric constants can be used in various analyses and carrier transport simulations. I was found, that oxygen vacancy can be both – electron and hole trap in HfO$_2$ and thus is possible to give a contribution in hafnia films conductivity.

References

[1] J. Robertson, Rep. Prog. Phys. 69 (2006) 327.
[2] V.V. Afanas'ev, A. Stesmans, Appl. Phys. Rev. 102 (2007) 081301.
[3] H.T. Takeuchi, T.-J. King, Appl. Phys. Lett. 83 (2003) 780–788.
[4] S.-G. Lim, S. Kriventsov, N. Jackson, et al., J. Appl. Phys. 91 (2002) 4500.
[5] M. Balog, M. Schieber, M. Michman, et al., Thin Solid Films 41 (1977) 247.
[6] X. Zhao, D. Vanderbilt, Phys. Rev. B 65 (2002) 233106.
[7] G.-M. Rignanese, X. Gonze, G. Jun, et al., Phys. Rev. B 69 (2004) 184301.
[8] J.L. Gavartin, D.M. Ramo, A.L. Shluger, et al., Appl. Phys. Lett. 89 (2006) 082908.
[9] P. Broqvist, A. Pasquarello, Appl. Phys. Lett. 89 (2006) 262904.
[10] K. Xiong, J. Robertson, M.C. Gibson, Appl. Phys. Lett. 87 (2005) 183505.
[11] H. Takeuchi, D. Ha, T.-J. King, J. Vac. Sci. Technol. A 22 (2004) 1337.
[12] D. Munoz Ramo, J.L. Gavartin, A.L. Shluger, Phys. Rev. B 75 (2007) 205336.